

**Technical Report
1201**

Boston Community Energy Study – Zonal Analysis for Urban Microgrids

**E.R. Morgan
S. Valentine
C.A. Blomberg
E.R. Limpaecher
E.V. Dydek**

5 April 2016

Lincoln Laboratory
MASSACHUSETTS INSTITUTE OF TECHNOLOGY
LEXINGTON, MASSACHUSETTS



This material is based upon work supported by the Department of Homeland Security,
Science and Technology Directory (DHS S&T) and the Department of Energy (DoE),
Office of Electricity Delivery and Energy Reliability (OE) under Air Force Contract No.
FA8721-05-C-0002 and/or FA8702-15-D-0001.

Approved for public release; distribution is unlimited.

This report is the result of studies performed at Lincoln Laboratory, a federally funded research and development center operated by Massachusetts Institute of Technology. This material is based on work supported by the Department of Homeland Security, Science and Technology Directorate (DHS S&T) under Air Force Contracts No. FA8721-05-C-0002 and/or FA8702-15-D-0001. Any opinions, findings and conclusions or recommendations expressed in this material are those of the authors and do not necessarily reflect the views of the DHS.

© (2016) MASSACHUSETTS INSTITUTE OF TECHNOLOGY

Delivered to the U.S. Government with Unlimited Rights, as defined in DFARS Part 252.227-7013 or 7014 (Feb 2014). Notwithstanding any copyright notice, U.S. Government rights in this work are defined by DFARS 252.227-7013 or DFARS 252.227-7014 as detailed above. Use of this work other than as specifically authorized by the U.S. Government may violate any copyrights that exist in this work.

**Massachusetts Institute of Technology
Lincoln Laboratory**

Boston Community Energy Study – Zonal Analysis for Urban Microgrids

*E.R. Morgan
S. Valentine
E.R. Limpaecher
E.V. Dydek
Group 73*

*C.A. Blomberg
Group 75*

Technical Report 1201

5 April 2016

Approved for public release; distribution is unlimited.

Lexington

Massachusetts

This page intentionally left blank.

ABSTRACT

Superstorm Sandy illustrated the economic and human impact that severe weather can have on urban areas such as New York City. While flooding and wind damaged or destroyed some of the energy infrastructure, all installed microgrids in the New York City region remained operational during Sandy, including those at Princeton University, Goldman Sachs, New York University, and Co-op City. The resilience provided by these microgrids sparked renewed interest in pursuing more microgrid deployments as means to increase resiliency throughout the nation and in the face of many potential threats including severe weather events, and potentially terrorism. MIT Lincoln Laboratory has been engaged with the Department of Homeland Security (DHS), the Department of Energy (DoE), and the City of Boston in this Community Energy Study to explore the potential for microgrid deployment within Boston's thriving neighborhoods. Using hourly simulated building energy data for every building in Boston, provided by the Sustainable Design Lab on MIT campus, MIT Lincoln Laboratory was able to develop an approach that can identify zones within the city where microgrids could be implemented with a high return on investment in terms of resiliency, offering both cost savings and social benefit in the face of grid outages. An important part of this approach leverages a microgrid optimization tool developed by Lawrence Berkeley National Laboratory, with whom the MIT Lincoln Laboratory is now collaborating on microgrid modeling work. Using the microgrid optimization tool, along with building energy use data, forty-two community microgrids were identified, including ten multiuser microgrids, ten energy justice microgrids, and twenty-two emergency microgrids.

This page intentionally left blank.

TABLE OF CONTENTS

	Page
Abstract	iii
List of Figures	vii
List of Tables	ix
 1. INTRODUCTION	 1
 2. MICROGRIDS	 3
2.1 Multiuser Microgrid	3
2.2 Energy Justice Microgrids	3
2.3 Emergency Microgrids	4
 3. MICROGRID PLACEMENT	 5
3.1 Underlying Data	5
3.2 Identifying sites as continuous thermal sinks	9
 4. DER-CAM PRIMER	 15
4.1 Cost Estimation in DER-CAM	16
4.2 DER-CAM Internal Data	18
 5. RESULTS	 21
5.1 Multiuser Microgrid	21
5.2 Affordable Housing Focused Energy Justice Microgrids and Emergency Microgrids	 27
 6. CONCLUSIONS	 33
 References	 35

This page intentionally left blank.

LIST OF FIGURES

Figure No.		Page
1	Building types in Boston.	6
2	Building vintages in Boston.	7
3	Building stock and associated energy use.	8
4	Diurnal energy use patterns in Boston.	9
5	Boston's hourly energy usage.	10
6	The top 0.2% of parcels in terms of total energy use.	11
7	Example microgrid zone analysis.	12
8	Identification of continuous thermal sinks.	13
9	Information flow for DER-CAM.	16
10	Normalized capital costs for discrete technologies in DER-CAM.	18
11	Radar plot of DER-CAM outputs.	19
12	Selected microgrid locations.	21
13	Base case assumptions for the MUMs.	22
14	MUM microgrid results against the base cases.	23
15	MUM cost and CO ₂ optimization.	25
16	Annual savings for MUMs.	25
17	Energy justice microgrid capacity vs. cost.	30
18	Energy justice microgrids capacity vs. savings.	31

This page intentionally left blank.

LIST OF TABLES

Table No.		Page
1	Economic Assumptions for Continuous Technologies in DER-CAM	17
2	MUM Cost Optimization Results	24
3	CO ₂ Optimization for MUMs	26
4	Base Case for the Energy Justice Microgrids	27
5	Cost Optimization for Energy Justice Microgrids	28
6	CO ₂ Optimization for Energy Justice Microgrids	29

This page intentionally left blank.

1. INTRODUCTION

According to the National Oceanic and Atmospheric Administration (NOAA), there were 178 weather events between 1980 and 2014 that exceeded \$1 billion in damages [1]. These events totaled more than \$1 trillion in costs, and took 9,179 lives. Large coastal cities are particularly vulnerable to weather events due to storm surge, high winds, and extreme precipitation. In 2012, New York City endured Superstorm Sandy, which killed 43 residents, and caused \$19 billion in damages [2], paralyzing the city and the surrounding area for days or weeks. In the wake of Superstorm Sandy, many states, including Maryland [3], New York [4], Massachusetts [5], and Minnesota [6], as well as the Federal Government [7], reassessed resilience to large-scale disasters, and the costs of being unprepared. Many of the reports focused on increasing resilience by employing urban microgrids that can island away from the larger grid and provide electricity to local markets. These microgrids typically exploit combined heat and power (CHP) systems to increase the overall energy efficiency, while increasing grid resilience. During Superstorm Sandy, all CHP units that were designed to operate autonomously in New York City and the surrounding area performed without incident [8]. By contrast, half of the backup generation systems in New York City hospitals failed during the Northeast blackout of 2003.

Microgrids can be leveraged to maintain normalcy during major catastrophes. During Superstorm Sandy, at least 11 facilities in the New York City area, representing over 145 MW of power, islanded from the macrogrid, and were able to provide critical infrastructure services [8]. These facilities included hospitals, waste water treatment facilities, colleges and universities, and large housing developments. Microgrids have a role in supporting critical infrastructures, and adding resilience to the local grid. Furthermore, microgrids can also add value to the macrogrid by providing ancillary services [9], thereby increasing overall reliability, and decreasing lost revenue [10].

Working with the Boston Redevelopment Authority (BRA), Massachusetts Institute of Technology Lincoln Laboratory (MIT LL) has completed a study to examine resilient power system design in Boston's thriving communities. The BRA is Boston's economic development and planning agency, responsible for attracting businesses to the greater Boston area. Energy system design is an emerging sector of community planning that involves many stakeholders and requires highly detailed data. Much of this data did not exist for small buildings and even many commercial buildings. The BRA identified this data gap and, through a request for proposal (RFP), instructed MIT Sustainable Design (SDL) Lab to create a Geographic Information Systems (GIS) enabled map of Boston showing the simulated energy use for each building for every hour of the year. Equipped with the simulated energy use in Boston, MIT Lincoln Laboratory was able to quickly analyze the potential technology solutions for improving resilience in multiple communities throughout the City. This component of the Community Energy Study is called the community energy simulation. The community energy simulation reflects certain policies of the City of Boston, including increasing affordability, increasing power grid resilience, and reducing greenhouse gas emissions.

MIT Lincoln Laboratory leveraged the simulated energy use data, along with geospatial analysis and a software package called Distributed Energy Resources Customer Adoption Model (DER-CAM) created by Lawrence Berkeley National Laboratory [11]. MIT Lincoln Laboratory generated maps and designs for over 30 different potential microgrid systems within the City of Boston. Each of these microgrid solutions came with unique designs to meet the energy needs of specific neighborhoods and communities based on certain policy criteria, as well as physical constraints. Upon the completion of the Boston energy research study, the City plans to use this information to enhance policy design and engage communities in dialogue about resilient energy system opportunities within their communities.

2. MICROGRIDS

Microgrids have no formal definition, but can generally be thought of as a local grouping of loads and generation that can operate either synchronously with the macrogrid or autonomously [12,13]. Synchronous operation typically implies that the microgrid is part of a larger power network, which could include other microgrids, or the macrogrid. Fully autonomous microgrids are ordinarily rural systems that have generation assets such as wind turbines (WTs) [14] or photovoltaic (PV) panels [15] that power loads such as lights and refrigeration. Microgrids consist of several components, including distributed generation (DG) for power production; energy storage, including for electricity, heat, and cooling; a master controller; and a utility grid interconnection [16,17]. The DG assets are typically low-voltage prime movers powered by internal combustion engines, diesel engines, microturbines, geothermal systems, hydro systems, or wind turbines; they also could include direct current devices such as fuel cells or photovoltaic arrays [6,17]. Traditional storage systems include electrical storage in batteries, heat storage, and cold storage [18].

Since many synchronous microgrids are adjacent to the loads that they are serving, there is an opportunity to provide both electricity and heat to the local community, thereby increasing the value of the purchased fuel. Many microgrids exploit this CHP concept, because the high thermal efficiency ($\approx 80\%$) translates into cost savings for the customers [19]. CHP systems are comprised of three major components: a prime mover, such as a gas turbine powered generator; heat exchangers for moving heat; and technologies such as absorption chillers that are thermally powered. CHPs are typically located on-site and provide some or all of the electricity demand alongside the thermal demands. Thus, under ideal situations, CHP can be used to provide nearly all of the required energy to a community, including electricity, heat, hot water, and cooling, assuming that the proper infrastructure – such as steam pipes for conveying heat – exists in the locality. This study focuses on three microgrid scenarios that aim to benefit the local community in different ways. The sections below discuss these three scenarios in more detail.

2.1 MULTIUSER MICROGRID

The multiuser microgrid (MUM) consists of local energy generation and the distribution of thermal and electric energy, and is a significant focus of the City of Boston. The MUM aims to replicate the energy systems of university and military campuses, but within commercial properties such as office buildings or within industrial areas. Because of the high building density, and therefore energy density, in Boston, each MUM is assumed to utilize CHP. In this way, MUMs can provide efficient fuel use, as well as utility grid services such as voltage support, load management, and ancillary services [20].

2.2 ENERGY JUSTICE MICROGRIDS

Energy justice microgrids focus on lowering the total cost of energy for communities in public housing. Very similar to MUMs, energy justice microgrids focus on affordable housing communi-

ties and surrounding critical facilities such as community shelters, grocery stores, and gas stations. These areas were identified using several GIS-enabled data sets, including Homeland Security Infrastructure Program (HSIP) gold and information from the BRA. The affordable housing data layer was intersected with several critical facilities layers to best determine suitable regions.

2.3 EMERGENCY MICROGRIDS

The design of an emergency microgrid is focused on maintaining critical infrastructure in times of electrical grid outage. Emergency microgrids are islands of reliability where communities can come to buy basic staples, charge cell phones, and escape extreme heat or cold. Moreover, they can provide basic shelter during natural disaster events.

The design includes local generation and – to the extent economically feasible – local distribution of heating and cooling. Emergency microgrids are similar to those microgrids found in Connecticut and those supported by Massachusetts Department of Energy Resources (DOER) Community Clean Energy Resiliency Initiative (CCERI) grant funding [21].

Emergency microgrids are anchored by the existing, designated community shelters in Boston that are co-located with grocery stores, convenience stores, gas stations, and other basic needs to keep residents safe during times of electrical grid outage.

3. MICROGRID PLACEMENT

Boston consists of about 112,000 separate buildings on 83,435 parcels of land, over an area of about 48 square miles; the estimated population of Boston in 2014 was 655,884 [22]. This section discusses the algorithm of siting a microgrid within this large Boston landscape, given the microgrid designs listed in the previous section, and data from both the City of Boston and the Sustainable Design Laboratory at MIT.

There are few works in the literature that focus on microgrid siting at the city level. The notable exceptions are a working paper from Columbia University that discusses spatiotemporal energy demands in New York City [23]. The model discussed in the working paper helps to inform an interactive block- and lot-level energy map of New York City [24]. A related study [25] showed the potential of CHP in Manhattan by simulating building energy use, and then employing an electric or thermal load following scheme to locate suitable areas for CHP. In general, the electric load following strategy for microgrid-level analysis identified 4714 microgrid CHP systems ranging in size from 100 kW to 2500 kW, representing an aggregated electrical capacity of 3042 MW. Another work studied a distributed local energy supply system in Tokyo [26]. The study used a 500 meter radius around a particular anchor load as its research area, finding that a microgrid would substantially help the surrounding community reduce CO₂ emissions and energy consumption. Finally, Finney et al. [27, 28] analyzed the expansion of district heating in Sheffield, United Kingdom on the city-scale, but did not consider the addition of microgrids to the area.

The present work uses a combination of the techniques presented in [23, 25, 26] to determine suitable microgrid zones throughout Boston. Simulated building energy use was used exclusively as the input for energy-based microgrid designs. Data layers such as the locations of substations, distribution lines, steam lines, and gas lines were not available for this analysis, which suggested a simple areal approach like the one used in [26]. However, since highly granular energy data was available, continuous thermal sinks – areas that constantly require heat, which could be supplied by a CHP plant – could be easily identified, much like the work done in [25, 27, 28].

3.1 UNDERLYING DATA

Boston has over 83,000 parcels of land that fall into about 20 different categories, ranging from office, to residential, to warehouse parcels, as determined by the City. All parcel types are shown in Figure 1, which does not show waterways or parks. The parcels are also divided into five vintages corresponding to the age of the coincident building on the parcel. The building vintages are shown in Figure 2, which illustrates that many of the oldest buildings in Boston are residential.

MIT Sustainable Design Lab developed an algorithm to generate energy use profiles for every parcel type in Boston [29]. The algorithm uses building type data in conjunction with building vintage data to better calculate the thermal envelope of buildings and estimate electricity usage. The energy use included plug load electricity – typical electrical loads such as lights or computers,

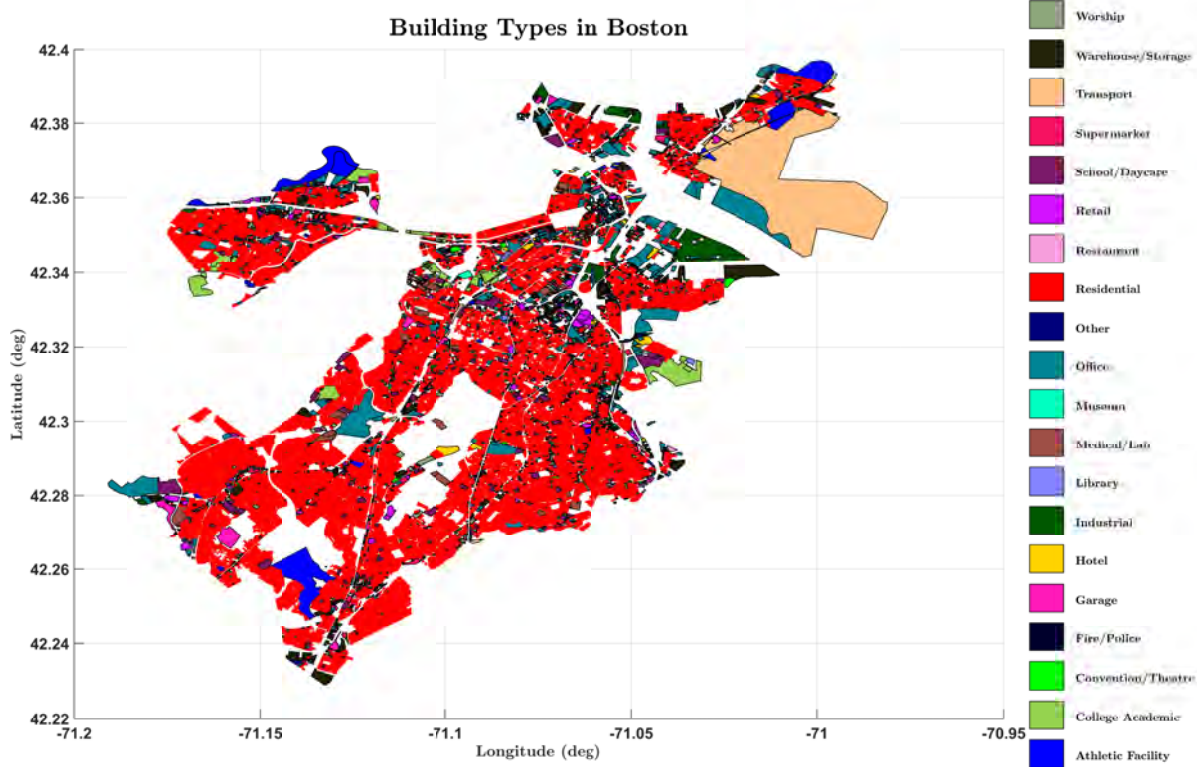


Figure 1. Building types in Boston.

cooling electricity, gas heating, and gas hot water were simulated for every hour of the year for each parcel in Boston. The resulting 60 GB data set was used as the basis for the analysis done by MIT Lincoln Laboratory.

Figure 1 elucidates how Boston's parcels are dominated by residential archetypes, which are depicted in red on the map. Figure 3 illustrates that residential parcels comprise more than 90% of all parcels in Boston, but represent only about 56% of the floor area. This indicates that while residential buildings are great in number, they are small in stature compared to office buildings, schools, colleges, and medical areas. In terms of energy demand, Figure 3 also demonstrates that per square meter, medical buildings, offices, and schools are intensive energy consumers relative to residential areas. Examples of high energy use are the medical community, which requires substantial cooling relative to its gross floor area, and hotels which use a disproportionate amount of hot water for their floor area.

Figure 4 illustrates how the four load types (plug load, cooling, etc.) differ across the seasons. The winter months in Boston are primarily dominated by heating loads, which peak in the morning hours. By contrast, the summer months have prevailing electrical and cooling loads that both have similar peak demands. Hot water loads are essentially the same for each season because they are

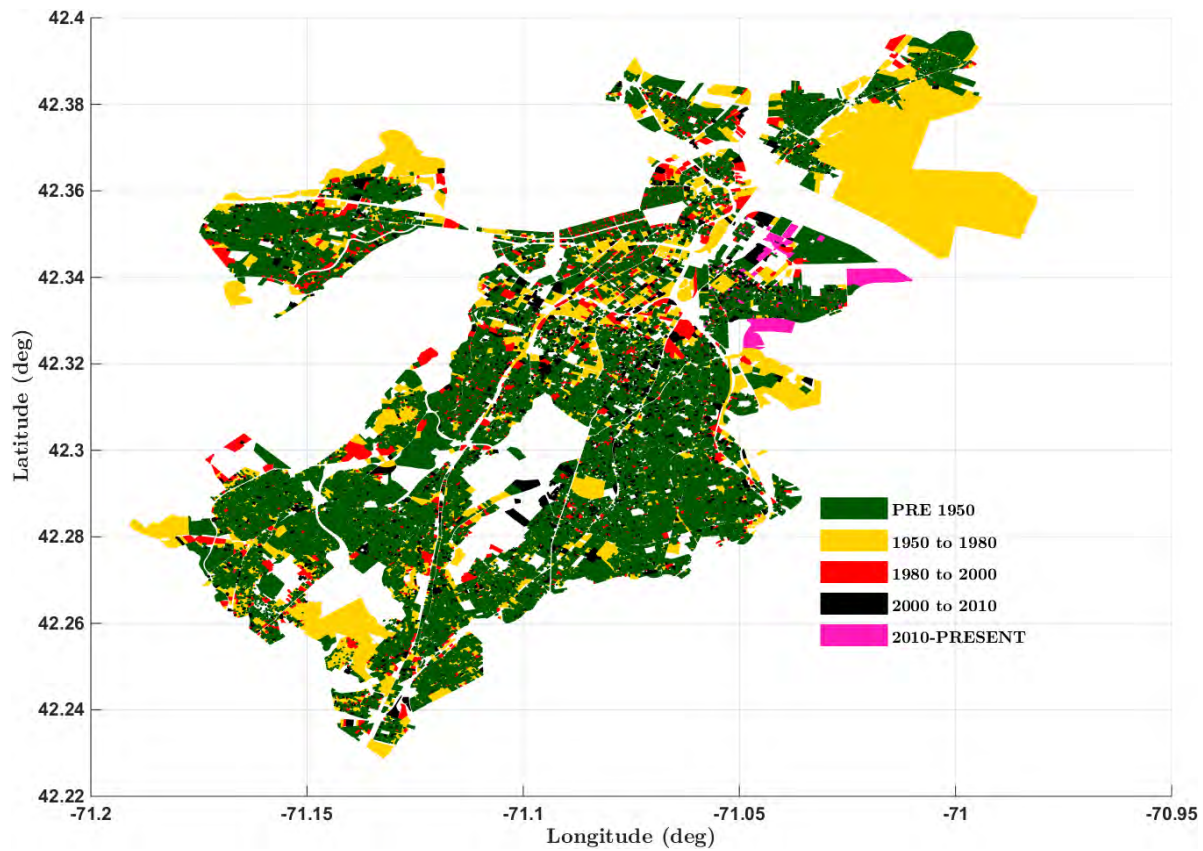


Figure 2. Building vintages in Boston.

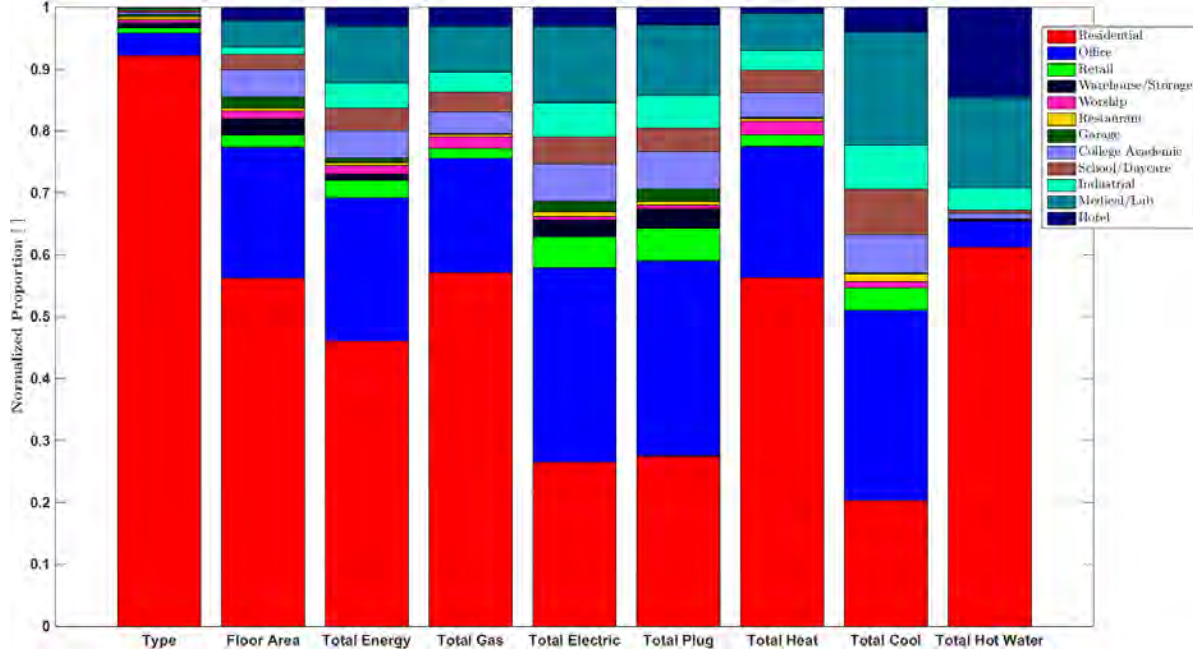


Figure 3. Building stock and associated energy use.

assumed to be dominated by morning and evening showering and bathing routines, which are not sensitive to the outdoor temperature.

A more granular energy representation can be made by aggregating the hourly energy data for all of Boston’s 83,000 parcels, and plotting it on a heat map. This map – shown in Figure 5 – demonstrates how the City uses energy for each hour of each day of the year. In the figure, the color is proportional to the energy use, which clearly explicates that the highest energy use occurs in the morning hours of January 23rd, a time when people are waking up, turning on lights, heating the home, and taking showers. The lowest energy use takes place in the early morning hours in early June, a time when few lights are on, people are generally sleeping, and no major heating or cooling loads are required. Thus, Boston’s energy use spans nearly two orders of magnitude in less than five months, where it switches from mostly gas heating in the winter to mostly electricity in the summer.

The energy data provided by the Sustainable Design Laboratory is extremely useful for a myriad of purposes. First, the data gives insight into how Boston operates – when it’s using gas versus using electricity and when it’s idling versus cooling. Second, it enables planners and policy makers to develop if/then scenarios that could be used to redesign the city, or to design future neighborhoods. Third, it gives a spatial sense of where Boston has energy bottlenecks, and where district energy systems would make sense: it gives highly valuable energy transparency. In the larger sense, the development of such high-quality, high-fidelity city-level energy models ushers in

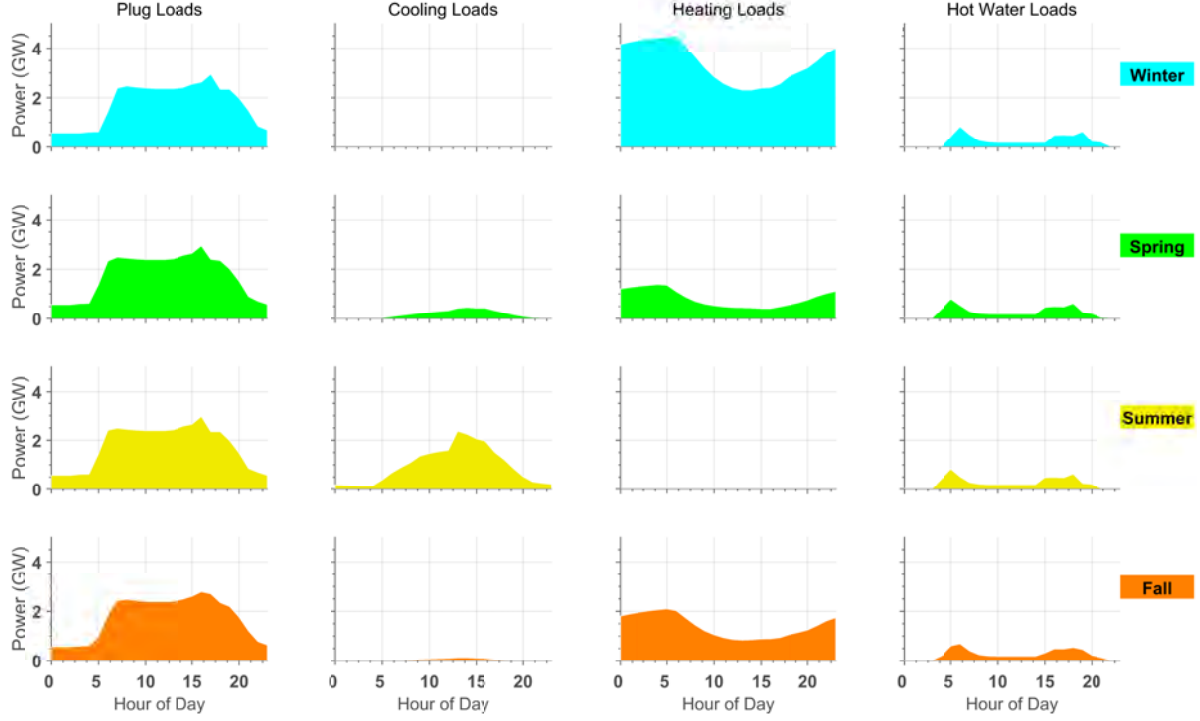


Figure 4. Diurnal energy use patterns in Boston.

a new paradigm of community planning that is relevant to many cities throughout the world.

MIT Lincoln Laboratory leveraged the simulated building energy data generated by MIT SDL to identify suitable microgrid zones throughout Boston. The microgrid zones were divided into three separate archetypes: multiuser microgrids, energy justice microgrids, and emergency microgrids, as discussed previously.

3.2 IDENTIFYING SITES AS CONTINUOUS THERMAL SINKS

A key starting point in the analysis is to identify buildings with a minimum threshold of high energy use that can serve as an “anchor building” for any microgrid. The role of the anchor building is to demand enough energy to justify the investment in local infrastructure upgrades; this makes infrastructure investment more palatable in the community and inspires other local stakeholders to consider becoming a part of the microgrid. From a modeling perspective, this necessitates identifying the top anchor buildings within the City of Boston and deriving microgrid zones of buildings from those key nodes. Figure 6 shows the top 0.2% (≈ 500) of parcels in Boston in terms of total annual energy use.

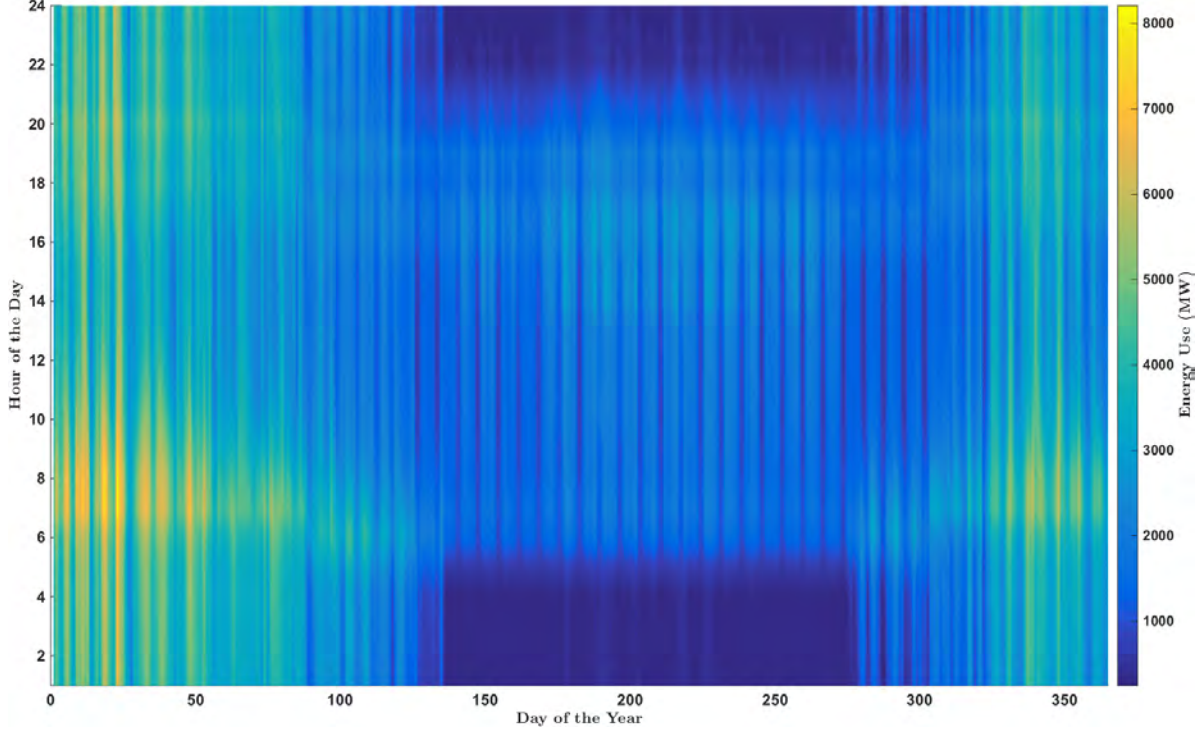


Figure 5. Boston's hourly energy usage.

The following design rule of thumb was implemented in the areas around each parcel to determine the suitability of a microgrid at that location [19, 30, 31]. Sixty percent of the electric load during peak week – the week with the highest average electricity demand – was used as the design size of the microgrid [32]. The CHP was assumed to have 40% fuel-to-electricity conversion efficiency, with the remaining 60% being waste heat. The algorithm is encapsulated in Equation 1. For each hour, the heat output from the CHP is compared to the simulated thermal requirements of the prospective microgrid zone. Zones that are capable of venting the CHP waste heat for the greatest number of hours annually are identified for closer scrutiny.

$$CHP_{Size} = \frac{3/5 \times \max(Elec_{avg, week})}{2/5} = \frac{3}{2} \times \max(Elec_{avg, week}) \quad (1)$$

Variably sized zones around anchor buildings were used to determine the most suitable size CHP plant for the particular anchor building, following the approach of [25]. Figure 7 shows a proposed microgrid zone, with the anchor building situated in the center. Concentric rings emanate out from the center point at increments of 50 meters, and the buildings that fall within the rings are considered for analysis. Thus, in this example, there are seven rings with the maximum radius being 350 meters, encompassing about 95 acres, and the minimum being 50 meters, encompassing about 2 acres. The energy usage of the buildings that fall within each circle are aggregated to determine

how well matched the thermal load requirements are with the electricity requirements. The results are presented in Figure 8. This analysis helped narrow down the prospective CHP sites from a myriad of possibilities. Other constraints were then added to further reduce the complexity. These constraints included:

- CHP sizes ranging from 10–50 MW
- No existing microgrid in the prospective zone
- Zone must include critical facilities such as supermarkets, pharmacies, gas stations, emergency shelters, and affordable housing

Implementing this rule of thumb for the top 0.2% of the highest energy use parcels within Boston, and applying the above constraints, ten nonoverlapping clusters were selected, each with a 250 meter radius for consistency. All of the selected 250 meter zones were determined to be thermal sinks on an annual basis.

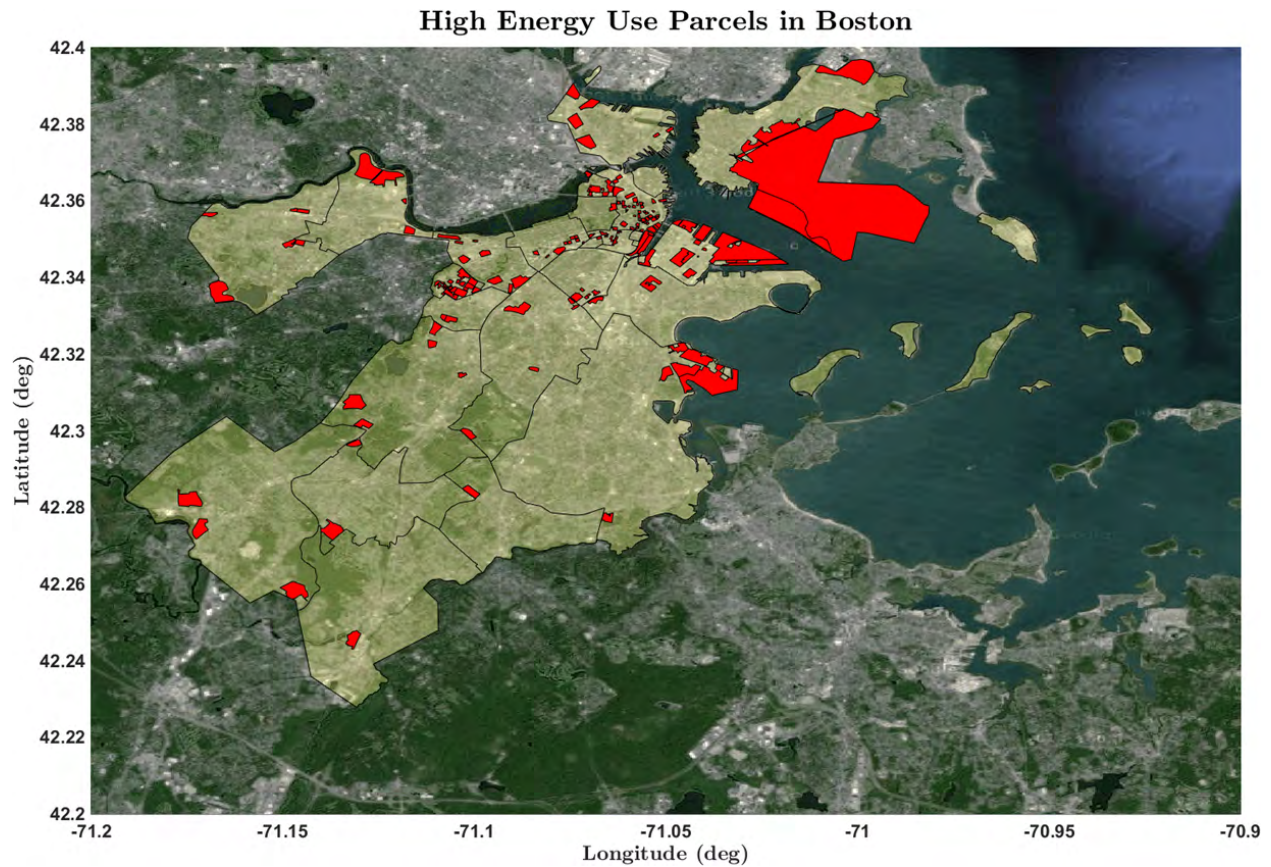


Figure 6. The top 0.2% of parcels in terms of total energy use.

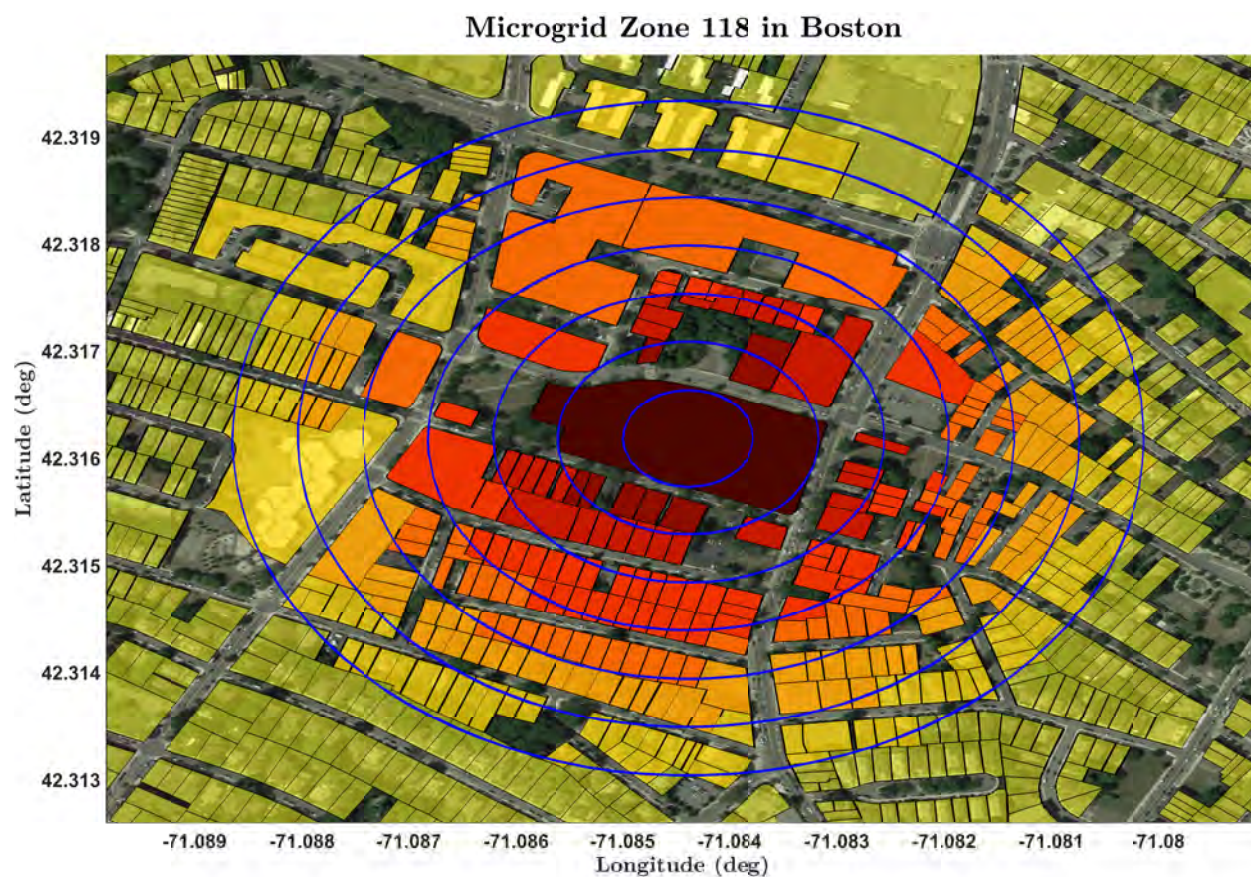


Figure 7. Example microgrid zone analysis.

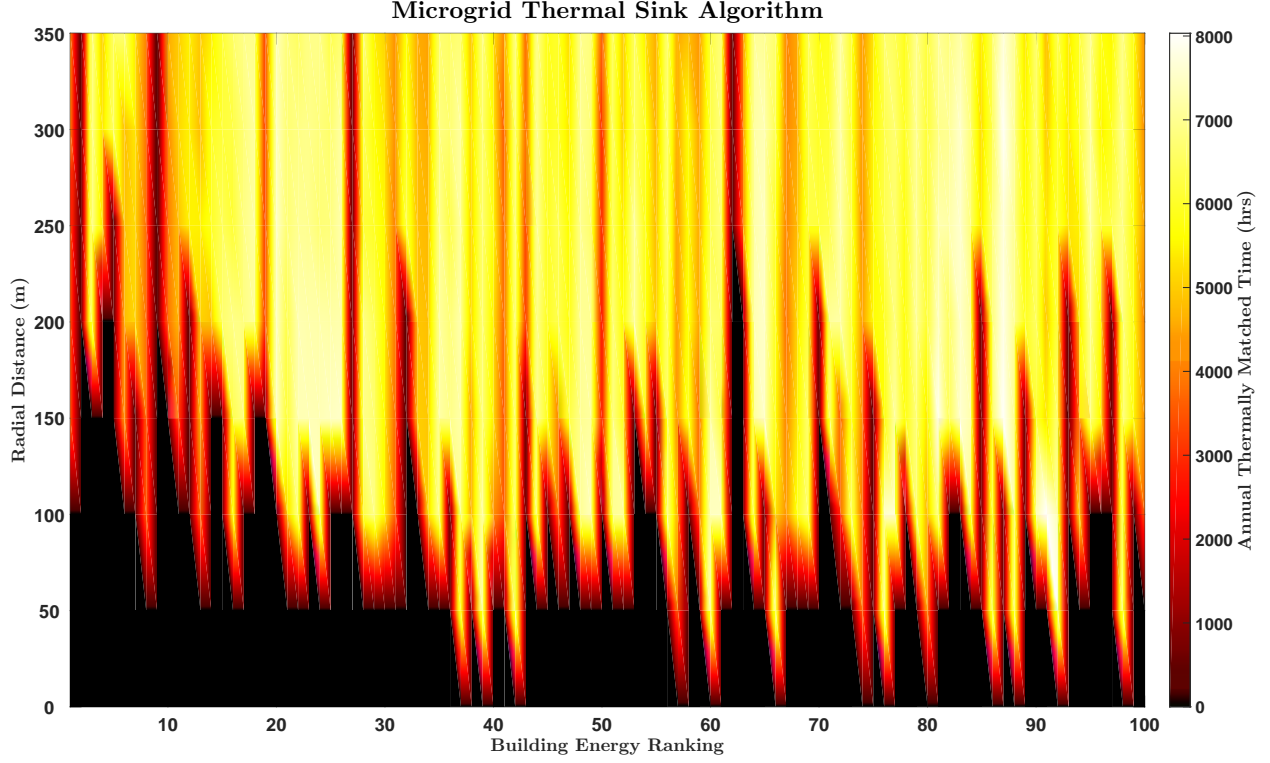


Figure 8. Identification of continuous thermal sinks.

The identification of appropriate microgrid zones is only one part of the problem. This strategy ultimately requires an assessment of the economic viability and environmental impact of microgrids in the prospective zones. Moreover, the optimal equipment mix and associated sizing along with the optimal dispatching strategy are also required for a full analysis. The Distributed Energy Resources Customer Adoption Model is a tool that allows us to quickly assess the suitability of microgrids in the identified zones. DER-CAM is discussed in the following section.

This page intentionally left blank.

4. DER-CAM PRIMER

The Distributed Energy Resources Customer Adoption Model (DER-CAM) was designed by Lawrence Berkeley National Laboratory to help inform decision makers who are seeking to add distributed energy resources to buildings or microgrids [11]. Using DER-CAM, the financial or environmental feasibility and suitability of the distributed generation can be determined. Figure 9 illustrates the DER-CAM optimization information flow, which is composed of:

1. Energy demand – hourly load profiles for heating, cooling, electricity, and hot water for weekdays and weekends
2. Utility prices – natural gas, electricity, oil, etc.
3. Local weather resources
4. Conventional storage and power conversion technology capital costs

Moreover, DER-CAM can also be instructed to disable or enable certain technologies or behavior, and can be given a set of operational constraints such as maximum generator size or available roof area for solar. These constraints effectively limit the search space of the optimization algorithm. The outputs from DER-CAM include the approximate costs and green house gas (GHG) emissions for the present situation (the base case), using cost optimization or CO₂ optimization or dual-objective cost and CO₂ optimization. When generating the optimal solution, DER-CAM not only obeys all impinging constraints, it also leverages performance and cost data from existing generation assets to arrive at the optimal solution.

In the present work, groups of buildings in Boston were identified as being potential microgrid zones. For each group of buildings, DER-CAM was used to calculate the base case annual costs and GHG emissions associated with the simulated energy usage data provided by MIT SDL. The GHG emissions were calculated using information from ISO New England (ISO-NE) regarding the power generation fleet, and standard values for emissions associated with fossil fuel technologies. The utility costs were calculated using utility pricing data and the simulated energy demand. The utility pricing data (electric and natural gas) was incorporated for three separate sectors, including industrial, residential, and commercial. The data was taken from the Energy Information Agency (EIA) for the latest year available [33]. DER-CAM was also utilized to determine the cost-optimal and CO₂-optimal scenarios which incorporated the energy demand, utility prices, local weather resources, and equipment capital costs.

Our analysis made several simplifying assumptions in order to reduce the complexity of the problem while still providing meaningful results. First, we assumed that equipment capital costs were the same for California and New England. Second, we assumed that there were no electricity demand charges, only electricity supply charges. Third, the electricity sales to the utility grid from a microgrid were disabled. Fourth, neither intra-building steam nor inter-building steam systems

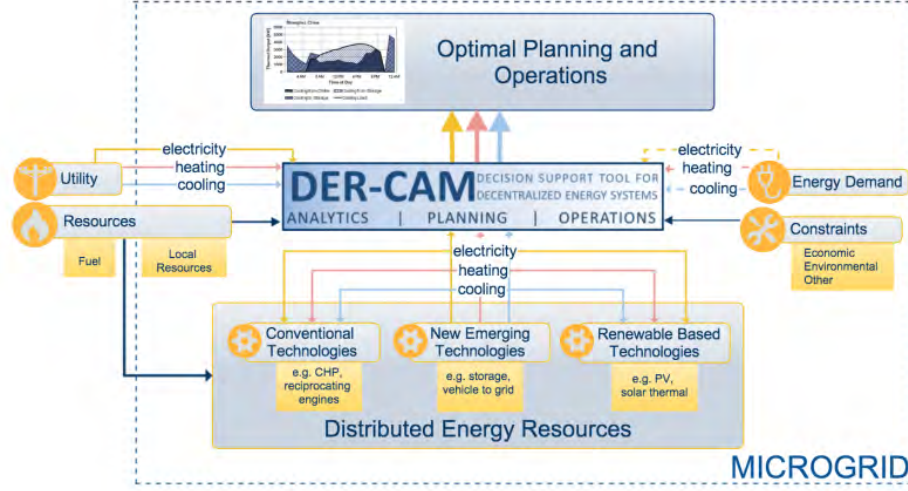


Figure 9. Information flow for DER-CAM.

were considered in the economic calculations; they were assumed to exist for the purposes of this study. In the aggregate, these assumptions streamline the calculations while maintaining the integrity of the results.

The capital costs for equipment are divided into two categories: discrete technologies, which are typically large pieces of equipment, such as gas turbines, that are only available in fixed sizes; and continuous technologies, such as PV panels, that can be aggregated to create a system of nearly any size. The discrete technologies and their associated capital costs and assumed lifetimes are provided in Table 1. Technologies of different sizes are assumed to have different normalized capital costs due to the economies of scale that are present in manufacturing the equipment. The assumptions for the continuous technologies are provided in Table 1. Here, the up-front cost must be paid whenever the technology is selected, regardless of size. This is akin to the commissioning costs, or permitting costs for a project. The normalized capital cost is given on a per-kilowatt or per-kilowatt hour basis, depending on the technology type. The lifetime and the assumed annual operations and maintenance costs (O&M) are also listed.

4.1 COST ESTIMATION IN DER-CAM

DER-CAM uses an internal library of predefined equipment capital costs to directly calculate the fixed annual costs associated with the CO_2 optimization and the cost optimization. The annual payment on the new capital equipment is assumed to be the product of the capital cost, C_c , and the capital recovery factor, CRF , as shown in Equation 2. The capital recovery factor is defined as the ratio of the constant annuity to the present value of receiving that annuity over n years, where n is the lifetime of the project, or equipment. Thus, using the effective interest rate, i , the CRF

TABLE 1

Economic Assumptions for Continuous Technologies in DER-CAM

Technology	Up-front Cost (\$)	Capital Cost (\$/kW or \$/kWh)	Lifetime (years)	O&M (%/year)
Heat Storage	10,000	50	17	0
Cold Storage	10,000	50	17	0
Battery	295	193	5	0
Absorption Chiller	93,900	685	20	1.88
Refrigeration	93,900	753	20	2.07
Photovoltaic	3,850	3,240	30	0.25
Solar Thermal	0	500	15	0.5
Air Source Heat Pump	0	70	10	0.52
Ground Source Heat Pump	0	80	10	0.32

is defined in Equation 3. For this analysis we incorporated an effective interest rate of 7% with a lifetime of 15 years, which is also assumed to be the project payback time.

$$P_a = C_c \times CRF \quad (2)$$

$$CRF = \frac{i}{1 - (1 + i)^{-n}} \quad (3)$$

Figure 10 portrays the capital costs of the discrete power conversion equipment, including microturbines (MTs), combustion turbines (CTs), and internal combustion engines. There are different cost curves for pieces of equipment that also include a combined heat and power (CHP) package, or a hot water (HW) package. The normalized capital costs decrease as the equipment gets larger, as predicted by the physics of scaling equipment, and the associated manufacturing capabilities [34]. For this analysis, all costs are assumed to be the ‘grass roots’ costs and include all necessary permitting, contingency, and installation costs [35].

DER-CAM uses all available discrete and continuous power conversion equipment in the optimization routine. The final technology selection is based upon the stated capital and O&M costs, lifetime, and stated payback time – set to 15 years for this analysis – for the power conversion equipment, as well as the existing utility prices and associated loads at the site. High equipment capital costs and/or operating costs paired with low existing costs could force DER-CAM to select the base case, rather than recommending any new technology.

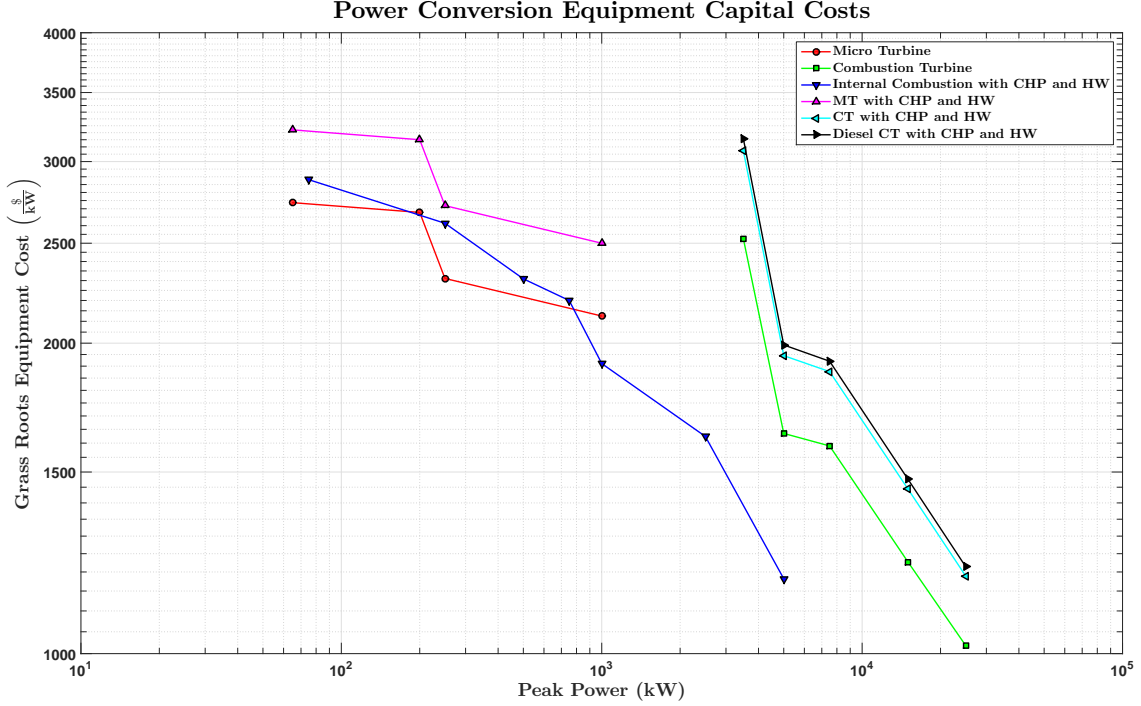


Figure 10. Normalized capital costs for discrete technologies in DER-CAM.

4.2 DER-CAM INTERNAL DATA

MIT Lincoln Laboratory obtained the source code for the DER-CAM platform from Lawrence Berkeley National Laboratory under a license agreement, so that DER-CAM could be better tailored to the Community Energy Study. MIT LL translated some of the internal parameters that DER-CAM uses to more accurately reflect regional cost and climate data. For example, the original version of DER-CAM uses average solar insolation values for San Francisco, which can be higher than those found in Boston by 25% [36]. The original version of DER-CAM also contains an internal library of temperature profiles for each month of the year, all based on typical meteorological year (TMY3) weather data for San Francisco [37]. Lincoln Laboratory updated these values using the TMY3 data for Logan Airport [37]. Finally, energy costs for New England were taken from the Energy Information Agency, including residential, industrial, and commercial pricing for both natural gas and electricity [38].

Figure 11 shows an example DER-CAM output set on a radar-style plot. The dotted green line shows the base case – how the buildings in the zone are performing now – for the microgrid zone. The red line denotes the DER-CAM cost optimization, while the blue line represents the CO₂ optimization results. The cost optimization run shows modest reduction in annual expenses versus both the base case and the CO₂ optimization. At the same time, the cost optimization also reduces the total CO₂ emissions from the base case. The CO₂ optimization, on the other hand, shows an

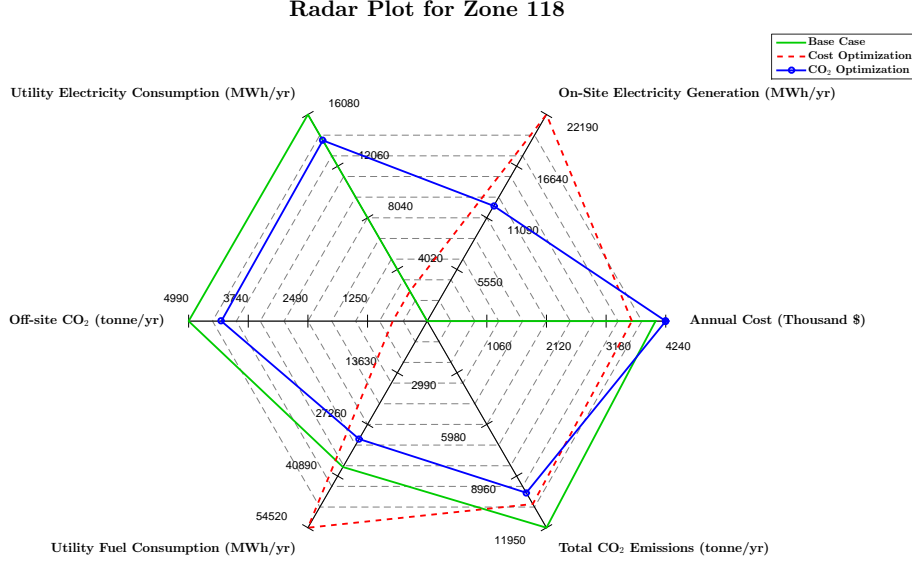


Figure 11. Radar plot of DER-CAM outputs.

increase in annual cost over the base case, but substantially reduces the total CO₂ emissions. The other four axes on the plot indicate how the system behaves:

1. Utility electricity consumption – the annual energy purchased from the grid
2. Off-site CO₂ generation – assuming the typical generation mix from ISO-NE
3. Utility fuel consumption – how much natural gas is typically purchased
4. On-site electricity generation – how much electricity is generated by the assets selected by DER-CAM

In totality, these six values indicate how distributed generation affects the financial and environmental performance of the buildings being served. In Figure 11, for example, both the cost and the CO₂ optimization reduce the CO₂ emissions when compared to the base case. Given that the cost optimization reduces the annual costs when compared to the base case, DER-CAM makes a compelling argument to invest in the cost optimal solution to reduce costs and emissions. The next section will further spell out the value that distributed generation can have in the urban environment in the context of three microgrid paradigms.

This page intentionally left blank.

5. RESULTS

This section explores three separate microgrid strategies that the City of Boston is promoting to improve energy resilience, while lowering energy costs and improving security. The three microgrid types were introduced and discussed in Section 2. For future reference in the following sections, Figure 12 presents a summary map of all selected microgrid zones for each microgrid strategy.

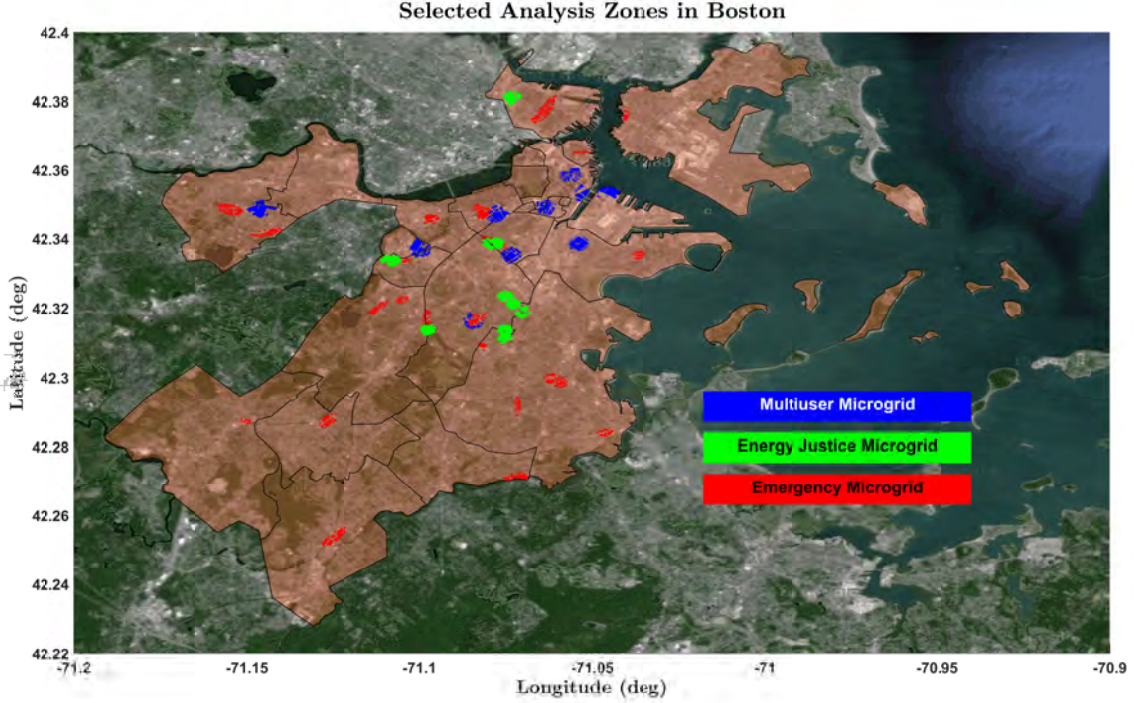


Figure 12. Selected microgrid locations.

5.1 MULTIUSER MICROGRID

The collections of buildings that were identified for the MUMs all include a large anchor load, with smaller loads aggregated from the surrounding area. The surrounding area was fixed at a radius of 250 meters, which was based on the thermal sink analysis that was done in Section 3.1. The aggregated simulated data for the building zones was used as an input to DER-CAM to determine the base case power requirements, costs, and estimated CO₂ emissions. The MUM base cases range in annual operating cost from a minimum of \$2.8 million to a maximum of \$36 million per year with average annual cost being about \$18 million. The average CO₂ emissions across the MUMs for the base case was calculated to be 48 kilotonnes of CO₂ equivalent. The results for each proposed MUM are presented in Figure 13.

Using DER-CAM to calculate the cost optimization scenario showed that an average savings per microgrid of 23.9% could be realized, equating to an average savings of \$4.35 million per year

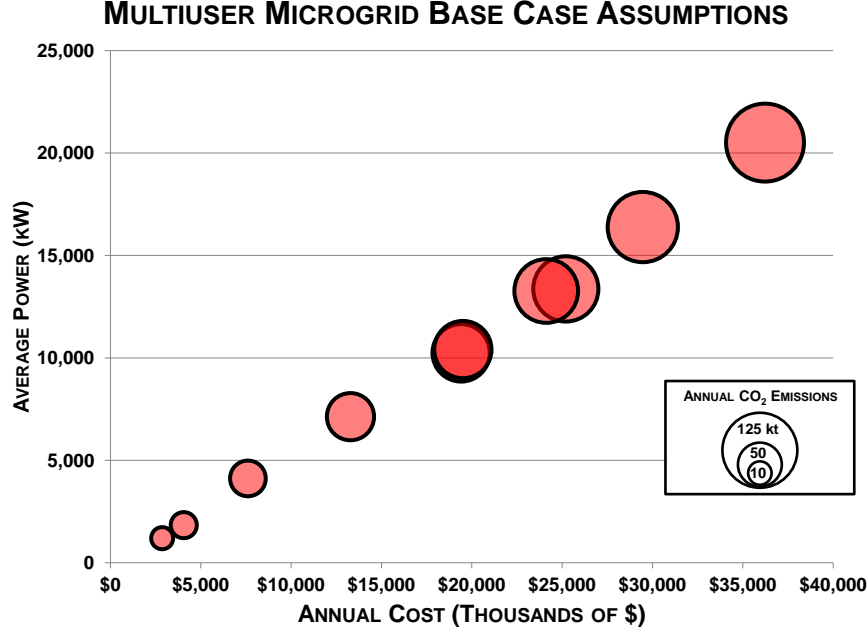


Figure 13. Base case assumptions for the MUMs.

per microgrid. The capital expenditure ranged from \$1 million to \$5.7 million, with an average capital expenditure of \$2.6 million. The average installed CHP capacity across the 10 analyzed microgrid zones was calculated to be just under 15 MW with a minimum CHP size of 2.5 MW and a maximum of 30 MW. Photovoltaic and solar thermal panels were largely adopted within each scenario, but were capped at 100 kW each due to roof area constraints. All microgrids were found to benefit from large air source heat pumps due to the low assumed capital costs ($\frac{\$70}{kW}$) and the favorable electricity generation from the CHP plants.

Figure 14 shows how the operating costs, energy consumption, and CO₂ emissions change versus the base case for both the cost optimization and the CO₂ optimization. In the cost optimization case, the operating costs and emissions are both lower at the expense of increased energy use. The increase in energy use is likely due to the favorable “spark spread” – the difference in price between electricity and the fuel used to produce the electricity. In Boston in 2014, the spark spread was about $\frac{\$70}{MWh}$, which is a significant fraction of the cost of electricity. This implies that it is advantageous to purchase fuel to produce electricity, and then dump the heat when it is not needed. These results indicate that higher overall energy consumption but lower bills. The energy consumption can be constrained by utilizing the CO₂ optimization which lowers the overall energy consumption at the expense of cost. The results suggest that a dual optimization approach should simultaneously reduce costs and GHG emissions.

Across all ten analyzed microgrid architectures, more than 90% of electricity could be potentially generated onsite under the cost-optimal scenario. CO₂ emissions savings were at a minimum

DER-CAM Results for All Multi-User Microgrid Zones

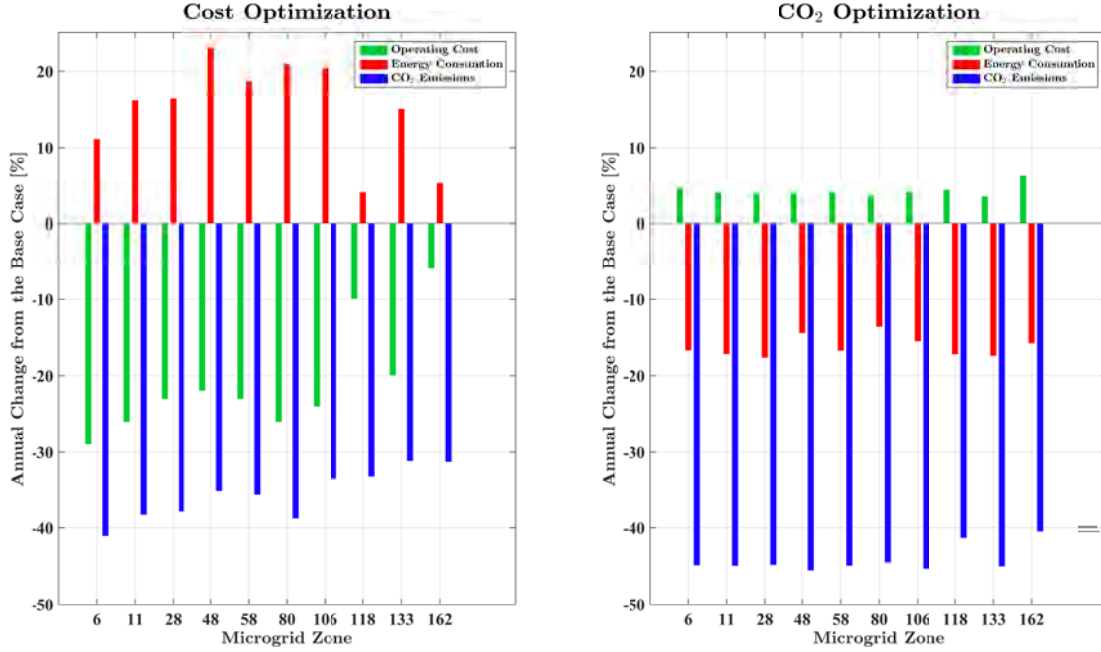


Figure 14. MUM microgrid results against the base cases.

of 4% against the base case, to a maximum of 12% with an average of 8% emissions saved. The cost optimization averages as well as the maximum and minimum values for the selected multiuser microgrids are provided in Table 2.

In the CO₂ optimization scenario, the operating costs increased by an average of 4% while both the energy consumption and the CO₂ emissions dropped across all analyzed zones by 16% and 45%, respectively. The range and capital expenditure was between \$1 million and \$5 million with an average of \$2.8 million spent on capital assets. Installed equipment included an average of 15 MW of combined heat and power with a minimum of 2500 kW and a maximum of 30 MW. All scenarios included some installed capacity for photovoltaic, or solar thermal technologies; all microgrids included air source heat pumps, with the average size approaching 20 MW. Finally, heat storage was employed in all microgrid zones except for zone 80, while cold storage was only found to be useful in two zones.

The results for the MUMs suggest that reductions in operating costs and CO₂ emissions are easily realizable in the selected microgrid zones. Moreover, there are likely many more zones in the City of Boston that could greatly benefit from a microgrid. Thus, Boston, and many other cities in the United States and the world, could benefit from microgrids and the and the cost and emissions reductions that they provide. Moving forward, this analysis shows that whenever new urban neighborhoods are being constructed, particularly in Boston, a microgrid design should at least be considered as the energy delivery system.

TABLE 2
MUM Cost Optimization Results

Scenario: Cost Optimization			
		Min	Max
Range of Op Costs	\$	2,696,000	28,129,000
Range in Savings	\$	168,000	8,095,000
Average Savings	\$	5,000,000	
Average % Savings		31.39%	
Range of Cap Ex	\$	960,000	5,702,000
Average Annualized Cap Ex	\$	263,000	
	Avg	Min	Max
Installed CHP Capacity [kW]	16,000	2,500	30,000
Photovoltaic [kW]	68	0	100
Solar Thermal [kW]	83	0	150
Air Source Heat Pump [kW]	8,233	2,125	15,918
Refrigeration [kW]	0	0	0
Electric Storage [kWh]	0	0	0
Heat Storage [kWh]	8,651	0	26,013
Cold Storage [kWh]	10,371	0	20,278
Absorption Chiller [kW]	1,148	0	3,253
Electricity Generated On-site [kWh/year]	93,225,000	14,687,000	182,252,000
	Avg	Min	Max
CO ₂ Emissions Savings [%]	8	4	12

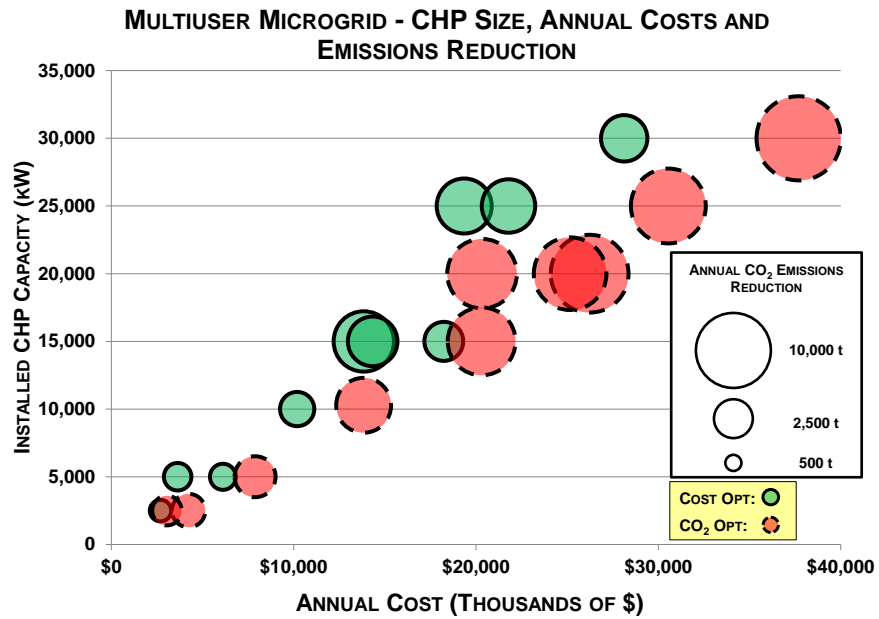


Figure 15. MUM cost and CO₂ optimization.

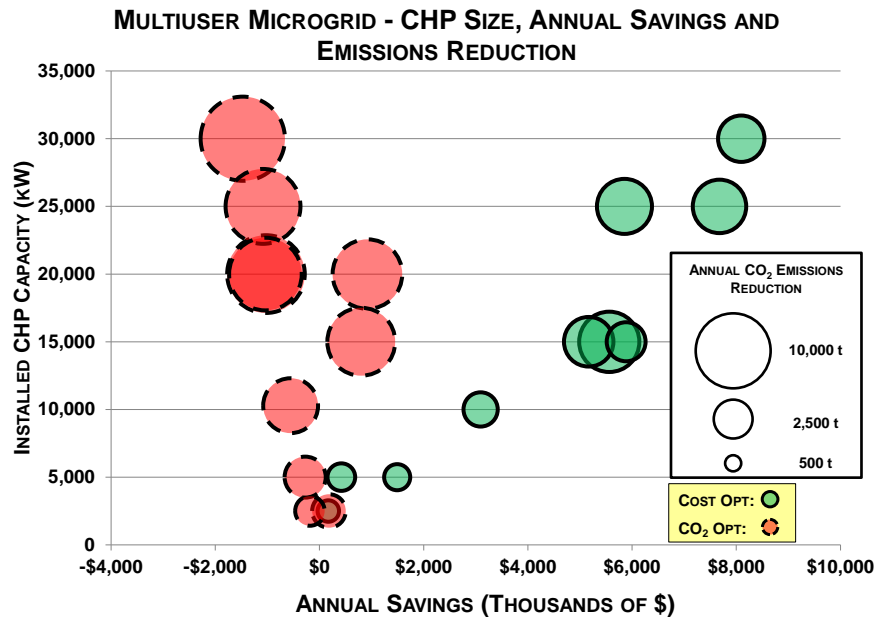


Figure 16. Annual savings for MUMs.

TABLE 3
CO₂ Optimization for MUMs

Scenario: CO ₂ Optimization			
		Min	Max
Range of Op Costs	\$	3,048,000	37,697,000
Range in Savings	\$	-2,143,000	-183,000
Average Savings	\$	-973,000	
Average % Savings		-3.98%	
Range of Cap Ex	\$	1,188,000	11,698,000
Average Cap Ex	\$	2,891,000	
	Avg	Min	Max
Installed CHP Capacity [kW]	15,028	2,500	30,000
Photovoltaic [kW]	85	0	133
Solar Thermal [kW]	225	0	750
Air Source Heat Pump [kW]	21,401	4,181	47,344
Heat Storage [kWh]	15,862	0	29,359
Cold Storage [kWh]	3,804	0	20,284
Absorption Chiller [kW]	0	0	0
Electricity Generated On-Site [MWh/year]	39,695	10,896	72,191
	Avg	Min	Max
CO ₂ Emissions Savings [kgCO ₂]	7,242,000	1,576,000	12,812,000

TABLE 4

Base Case for the Energy Justice Microgrids

Base Case			
		Min	Max
Range of Op Costs	\$	1,021,000	2,570,000
Average	\$	1,404,000	
Median	\$	1,335,000	
		Avg	Min
Annual CO ₂ Emissions (tonnes/yr)		3,947	2,976
			6,785

5.2 AFFORDABLE HOUSING FOCUSED ENERGY JUSTICE MICROGRIDS AND EMERGENCY MICROGRIDS

Two closely related microgrids scenarios are the energy justice and the emergency microgrids, each of which utilizes affordable housing information from the City of Boston. Both microgrid scenarios are designed to empower lower income residents, each in a different way. The energy justice microgrid seeks to reduce energy costs while increasing resiliency, whereas emergency microgrids provide basic health and shelter facilities. This section details the zone selection process and offers DER-CAM results for the energy justice microgrids.

5.2.1 Energy Justice Microgrids

The affordable housing energy justice microgrids were developed with the assistance of the affordable housing GIS layer, provided by the City of Boston. The most suitable energy justice zones were those that exhibited the highest density of affordable housing. The top ten zones with the highest affordable housing density (excluding dorms, such as those at UMass Boston) were selected for further analysis in DER-CAM. These zones are shown in Figure 12, alongside the multiuser microgrids and the emergency microgrids.

For the cost optimization scenario there were savings between \$692 annually and \$180,000 annually, with an average savings of 2.58%. Combined heat and power was a technology selected in most of the scenario outputs, while solar technologies were selected in all of them. For the CO₂ optimization, all energy justice zones were found to require CHP of 1 MW, with the exception of one zone that had a recommended capacity of 2 MW.

For an area this small it may be difficult to justify spending public or private capital on the distribution infrastructure required to link these buildings for a combined heat and power plant of a minimum of 1 MW. It is unclear if the efficiencies from the combined heat and power plant will outweigh the capital expenditure needed to create the piping network to link buildings together.

TABLE 5

Cost Optimization for Energy Justice Microgrids

Scenario: CO ₂			
		Min	Max
Range of Op Costs	\$	1,011,842	2,388,712
Range in Savings	\$	692	181,657
Average Savings		35,357	
Average % Savings		2.58%	
Range of Cap Ex	\$	377,551	680,893
Average Cap Ex	\$	484,949	
	Avg	Min	Max
Installed CHP Capacity [kW]	488	0	1,000
Photovoltaic [kW]	105	100	153
Solar Thermal [kW]	90	0	100
Air Source Heat Pump [kW]	415	0	950
Refrigeration [kW]	0	0	0
Electric Storage [kWh]	0	0	0
Heat Storage [kWh]	728	0	2,593
Cold Storage [kWh]	114	0	829
Absorption Chiller [kW]	14	0	142
Electricity Generated On-Site [kWh/year]	3,045,148	158,817	7,413,514
	Avg	Min	Max
CO ₂ Emissions Savings	8%	2%	16%

TABLE 6

CO₂ Optimization for Energy Justice Microgrids

Scenario: CO ₂			
		Min	Max
Range of Op Costs	\$	1,107,322	2,731,064
Range in Savings	\$	-160,694	-83,389
Average Savings		-94,781	
Average % Savings		-6.32%	
Range of Cap Ex	\$	611,679	794,673
Average Cap Ex	\$	677,998	
	Avg	Min	Max
Installed CHP Capacity [kW]	1,100	1,000	2,000
Photovoltaic [kW]	90	0	100
Solar Thermal [kW]	165	100	750
Air Source Heat Pump [kW]	1,787	1,074	3,327
Refrigeration [kW]	0	0	0
Electric Storage [kWh]	0	0	0
Heat Storage [kWh]	3,312	2,584	4,321
Cold Storage [kWh]	0	0	0
Absorption Chiller [kW]	0	0	0
Electricity Generated On-Site [kWh/year]	4,947,835	3,970,512	7,871,387
	Avg	Min	Max
CO ₂ Emissions Savings	21%	18%	23%

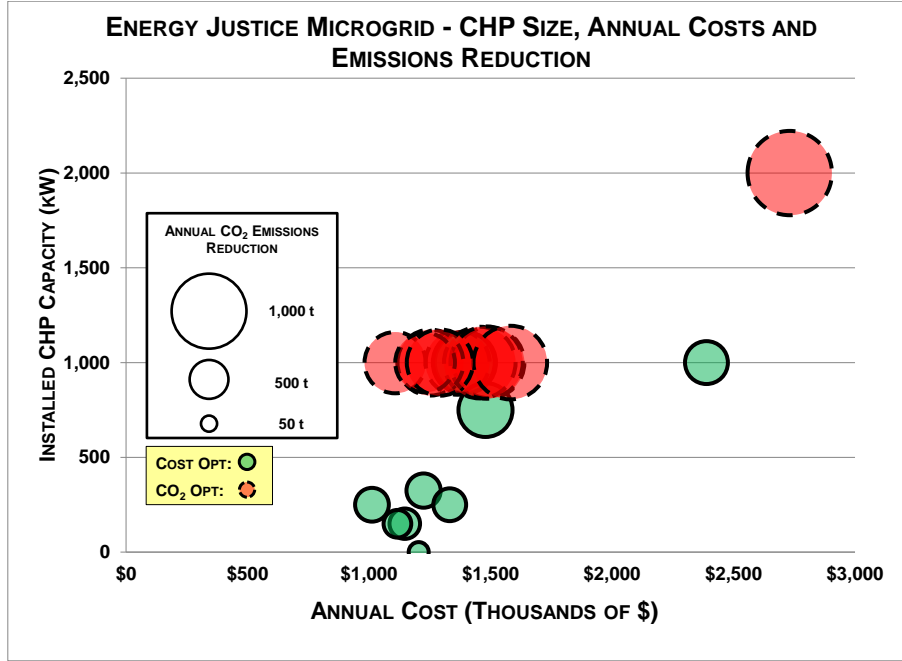


Figure 17. Energy justice microgrid capacity vs. cost.

For the CO₂ optimization scenario the range of costs included \$1.1 million to \$2.7 million with an average savings of -6.32%. This translates to spending more money on energy with the CO₂ optimization scenario. The capital expenditure ranges at a minimum of \$600,000 to \$800,000 at a maximum, with an average of \$677,000 spent on capital infrastructure.

Combined heat and power was largely utilized in every scenario, as were photovoltaics, solar thermal, air source heat pumps, and heat storage. A higher percentage of electricity was generated on-site, resulting in an annual output of 4,900 MWh per year. The CO₂ emissions savings range from 18% to 23% with an average of 21%. It would be difficult to justify to communities the increase in expenditure for carbon emissions reductions alone. Figure 12 shows the location of the energy justice microgrids identified as the most suitable in Boston.

5.2.2 Emergency Microgrids

The emergency microgrids also used affordable housing as the base layer, but included critical facilities in the selection calculus. These critical facilities were selected as places that the public could turn to for warmth, food, and water. For this analysis, the following critical facilities were considered:

- Emergency shelters

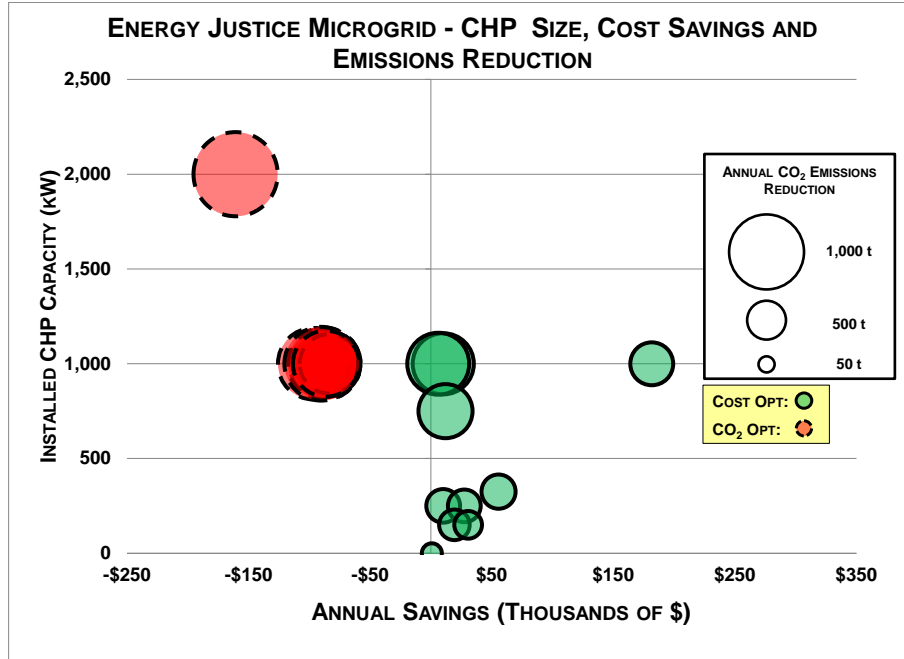


Figure 18. Energy justice microgrids capacity vs. savings.

- Gas/electric stations
- Pharmacies
- Supermarkets

The emergency shelters were further broken into the following list:

- Boston Centers for Youth and Families (BCYF)
- Colleges/universities
- Community centers
- Convention centers
- Cruise terminals
- Hotels/motels
- Libraries
- Museums
- Public schools

- Shelters
- Malls
- Baseball and football stadiums
- Basketball and hockey arenas

The affordable housing layer was intersected with the critical facility layer to determine suitable emergency microgrid locations. The areas with the highest population density and highest critical facility density were selected as sites to analyze further. The selected affordable housing buildings and critical facilities were aggregated into twenty-two different energy justice zones, as shown in Figure 12. Only two emergency microgrids were analyzed in DER-CAM, the average outputs of which are given in the Boston Community Energy Study report [39]. In the two analyzed emergency microgrids, the cost optimization showed that a average cost savings reduction of 13% is possible along with an average CO₂ reduction of 8%. The CO₂ optimization showed an average of 18% CO₂ reduction at the expense of a 6% cost increase.

6. CONCLUSIONS

The BRA, in conjunction with the MIT Sustainable Design Lab, MIT Lincoln Laboratory, energy consultants, and the developers of DER-CAM, successfully implemented a strategy for identifying microgrids across an entire city. This is the first-ever city-scale study of microgrids and the optimization of the energy delivery system in key neighborhoods and key buildings. The results suggest that microgrids can be used to reduce both costs and greenhouse gas emissions across a variety of Boston’s neighborhoods. Using the twenty-two suggested microgrids that were analyzed in DER-CAM, the BRA estimated that \$1 billion in cost and environmental savings is achievable over the next two decades. While the results generated by DER-CAM may be optimistic, they are compelling and certainly warrant further investigation. Moreover, this study is meant to begin a conversation with city planners, residents, and gas and electric utilities, rather than represent a definitive statement about where to build microgrids. The results show promising areas for further analysis and potential development, both for reducing costs and for reducing CO₂ emissions all while increasing the resilience of the overall grid.

This page intentionally left blank.

REFERENCES

- [1] National Oceanic and Atmospheric Administration, “Billion-Dollar Weather and Climate Disasters: Table of Events — National Centers for Environmental Information (NCEI),” (2015), <http://www.ncdc.noaa.gov/billions/events>.
- [2] PlaNYC - City of New York, “A stronger, more resilient New York,” PlaNYC, technical rep. (2013), http://s-media.nyc.gov/agencies/sirr/SIRR_singles_Lo_res.pdf.
- [3] A.R. Hopper, K. Lucas, D. Beugelmans, K. Haas, P. Bollinger, B. Carroll, and P. Dunbar, “Maryland resiliency through microgrids task force report,” State of Maryland, technical rep. (2014), http://energy.maryland.gov/Reports/MarylandResiliencyThroughMicrogridsTaskForceReport_000.pdf.
- [4] New York State Energy Research and Development Authority (NYSERDA), New York State Department of Public Service (DPS), and New York State Division of Homeland Security and Emergency Services (DHSES), “Microgrids for critical facility resiliency in New York State,” New York State Legislature, technical rep. 14–36 (2014).
- [5] KEMA Inc, “Microgrids – benefits, models, barriers and suggested policy initiatives for the Commonwealth of Massachusetts,” DNV KEMA, technical rep. (2014).
- [6] M.T. Burr, M.J. Zimmer, B. Meloy, J. Bertrand, W. Levesque, G. Warner, and J.D. McDonald, “Minnesota microgrids: Barriers, opportunities, and pathways toward energy assurance,” Microgrid Institute, technical rep. (2013).
- [7] President’s Council of Economic Advisers, U.S. Department of Energy’s Office of Electricity Delivery and Energy Reliability, and The White House Office of Science and Technology, “Economic benefits of increasing electric grid resilience to weather outages,” Executive Office of the President, technical rep. (2013).
- [8] A. Hampson, T. Bourgois, G. Dillingham, and I. Panzarella, “Combined heat and power: Enabling resilient energy infrastructure for critical facilities,” ICF International, technical rep. ORNL/TM-2013/100 (2013).
- [9] F. Farzan, S. Lahiri, M. Kleinberg, K. Gharieh, and M. Jafari, “Microgrids for fun and profit: The economics of installation investments and operations,” *Power and Energy Magazine, IEEE* 11(4), 52–58 (2013).
- [10] M.J. Sullivan, J. Schellenberg, and M. Blundell, “Updated value of service reliability estimates for electric utility customers in the United States,” Lawrence Berkeley National Laboratory, technical rep. LBNL-6941E (2015).
- [11] M. Stadler, D. Baldassari, T. Forget, S. Wagner, G. Cardoso, N. Deforest, L. Le Gall, C. Gehbauer, M. Hartner, S. Mashayekh, C. Milan, T. Schittekatte, D. Steen, and J. Tjaeder, “DER-CAM User Manual Full DER Web Optimization Service: A project partly financed by

- the U.S. Department of Energy,” Lawrence Berkeley National Laboratory (LBNL), technical rep. (2015), https://building-microgrid.lbl.gov/sites/all/files/DER-CAM_User_Manual_v1_Rev2.pdf.
- [12] Z. Ye, R. Walling, N. Miller, P. Du, and K. Nelson, “Facility microgrids,” National Renewable Energy Laboratory, technical rep. NREL/SR-560-38019 (2005).
 - [13] R. Lasseter, “Microgrids,” in *Power Engineering Society Winter Meeting. IEEE* (2002), vol. 1, pp. 305–308.
 - [14] G. Notton, M. Muselli, P. Poggi, and A. Louche, “Decentralized wind energy systems providing small electrical loads in remote areas,” *International Journal of Energy Research* 25(2), 141–164 (2001), <http://dx.doi.org/10.1002/er.670>.
 - [15] A. Celik, “The system performance of autonomous photovoltaic – wind hybrid energy systems using synthetically generated weather data,” *Renewable Energy* 27(1), 107–121 (2002), <http://www.sciencedirect.com/science/article/pii/S0960148101001689>.
 - [16] C.L. Smallwood, “Distributed generation in autonomous and nonautonomous microgrids,” in *Rural Electric Power Conference. IEEE*, IEEE (2002), pp. D1–D1.6.
 - [17] N. Hatziargyriou, H. Asano, R. Iravani, and C. Marnay, “Microgrids,” *Power and Energy Magazine, IEEE* 5(4), 78–94 (2007).
 - [18] M. Stadler, “Effect of Heat and Electricity Storage and Reliability on Microgrid Viability: A Study of Commercial Buildings in California and New York States.” Lawrence Berkeley National Laboratory., technical rep. (2009), <http://escholarship.org/uc/item/2p0526g5>.
 - [19] Midwest CHP Application Center and Avalon Consulting, “Combined Heat and Power (CHP) Resource Guide,” Midwest CHP Application Center (2005), <http://smartenergy.illinois.edu/pdf/archive/chpresourceguide2003sep.pdf>.
 - [20] C. Villarreal, D. Erickson, and M. Zafar, “Microgrids: A regulatory perspective,” California Public Utilities Commission - Policy & Planning Division, technical rep. (2014).
 - [21] D. Beavers, D. Burns, C. McClelland, and R. Fahey, “Final report: Community clean energy resiliency initiative,” The Cadmus Group (2015), <http://www.mass.gov/eea/docs/doer/renewables/resiliency/cceri-final-report.docx>.
 - [22] United States Census Bureau, “American factfinder - community facts,” (2015), http://factfinder.census.gov/faces/nav/jsf/pages/community_facts.xhtml.
 - [23] L. Parshall, H. Jónsdóttir, S.A. Hammer, and V. Modi, “Spatio-temporal patterns of energy demand in New York City and implications for cogeneration,” (2010), http://sallan.org/EventPix_slideshow_Smart-Grid/resources/L-Parshall_NYC_Cogen_WorkingPaper_Jan2010.pdf.

- [24] B. Howard, L. Parshall, J. Thompson, S. Hammer, J. Dickinson, and V. Modi, “Estimated Total Annual Building Energy Consumption at the Block and Lot Level for New York City,” (2015), <http://sel-columbia.github.io/nycenergy/>.
- [25] B. Howard, A. Saba, M. Gerrard, and V. Modi, “Combined heat and power’s potential to meet New York City’s sustainability goals,” *Energy Policy* 65, 444–454 (2014), <http://www.sciencedirect.com/science/article/pii/S0301421513010550>.
- [26] H. Chen, R. Ooka, K. Iwamura, H. Huang, N. Yoshizawa, K. Miisho, S. Yoshida, S. Namatame, A. Sakakura, and S. Tanaka, “Study on sustainable redevelopment of a densely built-up area in Tokyo by introducing a distributed local energy supply system,” *Energy and Buildings* 40(5), 782–792 (2008), <http://www.sciencedirect.com/science/article/pii/S0378778807001703>.
- [27] K.N. Finney, V.N. Sharifi, J. Swithenbank, A. Nolan, S. White, and S. Ogden, “Developments to an existing city-wide district energy network, Part I: Identification of potential expansions using heat mapping,” *Energy Conversion and Management* 62, 165–175 (2012), <http://www.sciencedirect.com/science/article/pii/S019689041200132X>.
- [28] K.N. Finney, Q. Chen, V.N. Sharifi, J. Swithenbank, A. Nolan, S. White, and S. Ogden, “Developments to an existing city-wide district energy network, Part II: Analysis of environmental and economic impacts,” *Energy Conversion and Management* 62, 176–184 (2012), <http://www.sciencedirect.com/science/article/pii/S0196890412001318>.
- [29] C.C. Davila, C. Reinhart, and J. Bemis, “Modeling boston: A workflow for the generation of complete urban building energy demand models from existing urban geospatial datasets,” (2015), http://web.mit.edu/SustainableDesignLab/projects/BostonEnergyModel/_doc/CWES_MIT_SDL_NOV15.pdf.
- [30] Action Energy, “Combined heat and power for buildings - selecting, installing and operating CHP in buildings – a guide for building services engineers,” Carbon Trust, technical rep. (2004), <http://files.harc.edu/Sites/GulfCoastCHP/ProjectDevelopment/UKGoodPracticeGuide.pdf>.
- [31] Midwest CHP Application Center, “Combined Heat & Power (CHP) Resource Guide for Hospital Applications,” technical rep. (2007), https://www.wbdg.org/ccb/VA/VASUSTAIN/chp_hospital_guidebook.pdf.
- [32] J.J. Cuttica and C. Haefke, “Combined Heat and Power (CHP) – Is It Right For Your Facility,” (2015), http://energy.gov/sites/prod/files/2013/11/f4/webcast_2009-0514_chp_in_facilities.pdf.
- [33] Energy Information Administration, “U.S. energy information administration - data,” (2015), <http://www.eia.gov/electricity/data.cfmsales>.
- [34] G. Ulrich, *A Guide to Chemical Engineering Process Design and Economics*, Wiley (1984), <https://books.google.com/books?id=pdVTAAAAMAAJ>.

- [35] R. Turton, R. Bailie, W. Whiting, J. Shaeiwitz, and D. Bhattacharyya, *Analysis, Synthesis and Design of Chemical Processes*, Prentice Hall International Series in the Physical and Chemical Engineering Sciences, Pearson Education (2012), https://books.google.com/books?id=R_olxZYJWQoC.
- [36] National Renewable Energy Laboratory, “NREL: Dynamic Maps, GIS Data, and Analysis Tools - Solar Maps,” (2015), <http://www.nrel.gov/gis/solar.html>.
- [37] National Renewable Energy Laboratory, “NSRDB: 1991–2005 - Update,” (2015), http://rredc.nrel.gov/solar/old_data/nsrdb/1991-2005/tmy3/.
- [38] U.S. Energy Information Administration, “Energy Information Administration – EIA – official energy statistics from the U.S. Government,” (2015), <http://www.eia.gov/naturalgas/data.cfm>.
- [39] Boston Redevelopment Authority Planning Division, “Boston Community Energy Study: Exploring the Potential for Local Energy Generation, District Energy, and Microgrids,” Boston Redevelopment Authority, technical rep. (2016).

REPORT DOCUMENTATION PAGE				Form Approved OMB No. 0704-0188	
Public reporting burden for this collection of information is estimated to average 1 hour per response, including the time for reviewing instructions, searching existing data sources, gathering and maintaining the data needed, and completing and reviewing this collection of information. Send comments regarding this burden estimate or any other aspect of this collection of information, including suggestions for reducing this burden to Department of Defense, Washington Headquarters Services, Directorate for Information Operations and Reports (0704-0188), 1215 Jefferson Davis Highway, Suite 1204, Arlington, VA 22202-4302. Respondents should be aware that notwithstanding any other provision of law, no person shall be subject to any penalty for failing to comply with a collection of information if it does not display a currently valid OMB control number. PLEASE DO NOT RETURN YOUR FORM TO THE ABOVE ADDRESS.					
1. REPORT DATE (DD-MM-YYYY) 5 April 2016		2. REPORT TYPE Technical Report		3. DATES COVERED (From - To)	
4. TITLE AND SUBTITLE Boston Community Energy Study – Microgrid Zonal Analysis				5a. CONTRACT NUMBER FA8721-05-C-0002 and/or FA8702-15-D-0001	
				5b. GRANT NUMBER	
				5c. PROGRAM ELEMENT NUMBER	
6. AUTHOR(S) Eric R. Morgan, Stephen Valentine, Cheryl A. Blomberg, Erik R. Limpaecher, and E. Victoria Dydek				5d. PROJECT NUMBER 10163	
				5e. TASK NUMBER 31	
				5f. WORK UNIT NUMBER	
7. PERFORMING ORGANIZATION NAME(S) AND ADDRESS(ES) MIT Lincoln Laboratory 244 Wood Street Lexington, MA 02420-9108				8. PERFORMING ORGANIZATION REPORT NUMBER TR-1201	
9. SPONSORING / MONITORING AGENCY NAME(S) AND ADDRESS(ES) Department of Homeland Security, Science and Technology Directorate Jalal Mapar 245 Murray Lane, SW Washington, DC 20528				10. SPONSOR/MONITOR'S ACRONYM(S) DHS (S&T)	
				11. SPONSOR/MONITOR'S REPORT NUMBER(S)	
12. DISTRIBUTION / AVAILABILITY STATEMENT Distribution Statement A: Approved for public release; distribution is unlimited.					
13. SUPPLEMENTARY NOTES					
14. ABSTRACT Superstorm Sandy illustrated the economic and human impact that severe weather can have on urban areas such as New York City. While flooding and wind damaged or destroyed some of the energy infrastructure, all installed microgrids in the New York City region remained operational during Sandy, including those at Princeton University, Goldman Sachs, New York University, and Co-op City. The resilience provided by these microgrids sparked renewed interest in pursuing more microgrid deployments as means to increase resiliency throughout the nation and in the face of many potential threats including severe weather events, and potentially terrorism. MIT Lincoln Laboratory has been engaged with the Department of Homeland Security (DHS), the Department of Energy (DoE), and the City of Boston in this Community Energy Study to explore the potential for microgrid deployment within Boston's thriving neighborhoods. Using hourly simulated building energy data for every building in Boston, provided by the Sustainable Design Lab on MIT campus, MIT Lincoln Laboratory was able to develop an approach that can identify zones within the city where microgrids could be implemented with a high return on investment in terms of resiliency, offering both cost savings and social benefit in the face of grid outages. An important part of this approach leverages a microgrid optimization tool developed by Lawrence Berkeley National Laboratory, with whom the MIT Lincoln Laboratory is now collaborating on microgrid modeling work. Using the microgrid optimization tool, along with building energy use data, forty-two community microgrids were identified, including ten multiuser microgrids, ten energy justice microgrids, and twenty-two emergency microgrids.					
15. SUBJECT TERMS					
16. SECURITY CLASSIFICATION OF:			17. LIMITATION OF ABSTRACT Same as report	18. NUMBER OF PAGES 48	19a. NAME OF RESPONSIBLE PERSON
a. REPORT Unclassified	b. ABSTRACT Unclassified	c. THIS PAGE Unclassified			19b. TELEPHONE NUMBER (include area code)